Synthesis and treatment of biosorbent from cyanobacterial biomass for the removal of NO_3^--N from aqueous systems

George Mazarakos[a], Christina Vasiliki Lazaratou[a*], Zacharias Frontistis[b], Athanasia G. Tekerlekopoulou[c], Vasilios Georgakilas[d], Dimitris V. Vayenas[a,e]

[a]Department of Chemical Engineering, University of Patras, GR-26504 Patras, Greece

[b]Department of Chemical Engineering, University of Western Macedonia, GR-50132, Kozani, Greece

[c]Department of Sustainable Agriculture, University of Patras, 30100 Agrinio, Greece

[d]Department of Materials Science, School of Natural Sciences, University of Patras, Patras, 26504, Greece

[e]Institute of Chemical Engineering Sciences, Foundation for Research and Technology, PO Box 1414, GR -26504 Patras, Greece

*corresponding author: c.lazaratou@ac.upatras.gr

Supplementary material

List of Figures

Figure S1: Calibration curve of $NO_3^- - N$ according to the 4500- NO_3^- -B method.
Figure S2 ζ-potential as a function of pH for biomass and hydrochar (isoelectric point).
Figure S3: Illustration of the removal efficiency of $NO_3^- - N$ as a function of time for each adsorption experiment performed by using the modified hydrochar ($V = 0.15\ L, pH = 6.5, = 25$ ℃).
Figure S4: Removal efficiencies paired with adsorption capacities of all examined adsorbent dosages
Figure S5: Removal efficiencies paired with adsorption capacities of all examined Initial $NO_3^- - N$ concentrations
Figure S6: Illustration of the non-linear forms of the pseudo-first-order and pseudo-second-order models: (a) at different adsorption dosages of biomass, and (b) at different initial concentrations of NO_3^--N using biomass as the adsorbent.
Figure S7: Illustration of the non-linear forms of the pseudo-first-order and pseudo-second-order models: (a) at different adsorption dosages of biomass, and (b) at different initial concentrations of NO_3^--N using hydrochar as the adsorbent.

List of Tables

Table S1: Complete kinetic parameters obtained by non-linear regression for the pseudo-first-order (PFO) and pseudo-second-order (PSO) models. The table presents the correlation coefficient R^2), residual sum of squares (RSS), and calculated equilibrium capacity (qe) for nitrate removal by biomass and hydrochar

Table S2: Parameters for the Langmuir, Freundlich, and Dubinin-Radushkevich isotherm models obtained by non-linear regression for nitrate removal by biomass and hydrochar

Table S3: Parameters for the Adams-Bohart column adsorption model obtained by non-linear fitting to the initial breakthrough region for biomass and hydrochar fixed-bed columns.

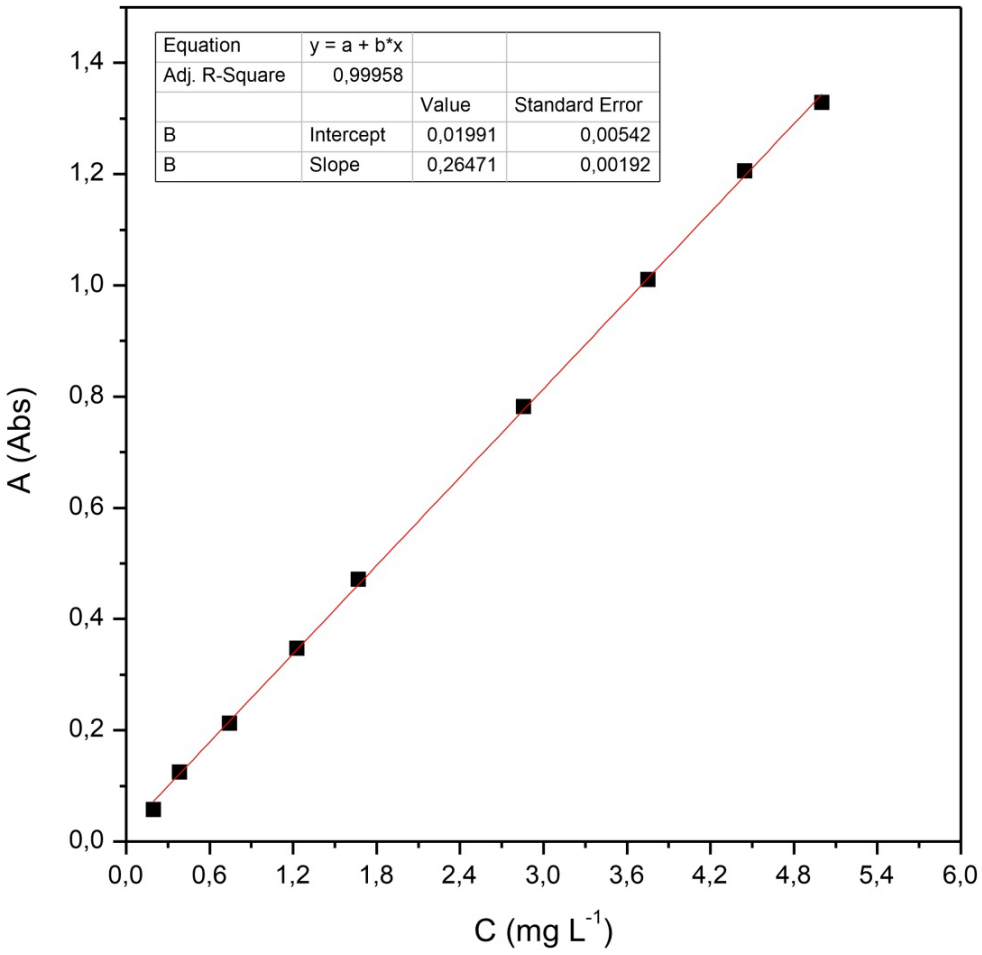


Figure S1: Calibration curve of $NO_3^- - N$ according to the 4500- NO_3^- -B method.

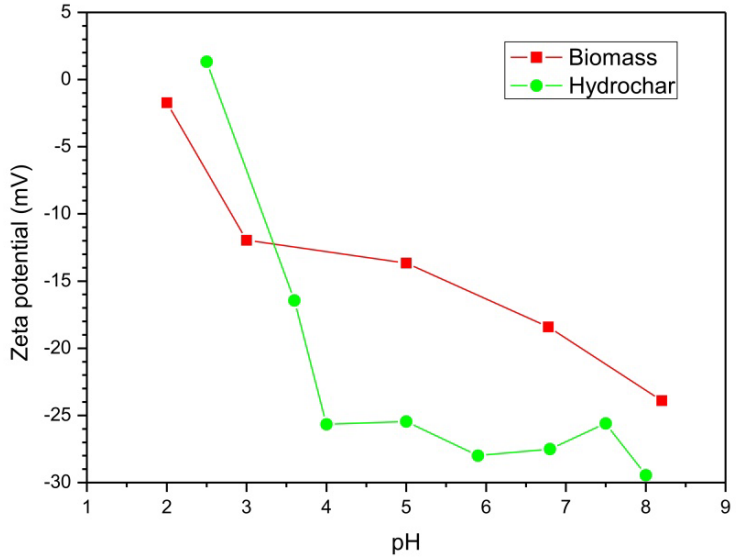


Figure S2: ζ-potential as a function of pH for biomass and hydrochar (isoelectric point).

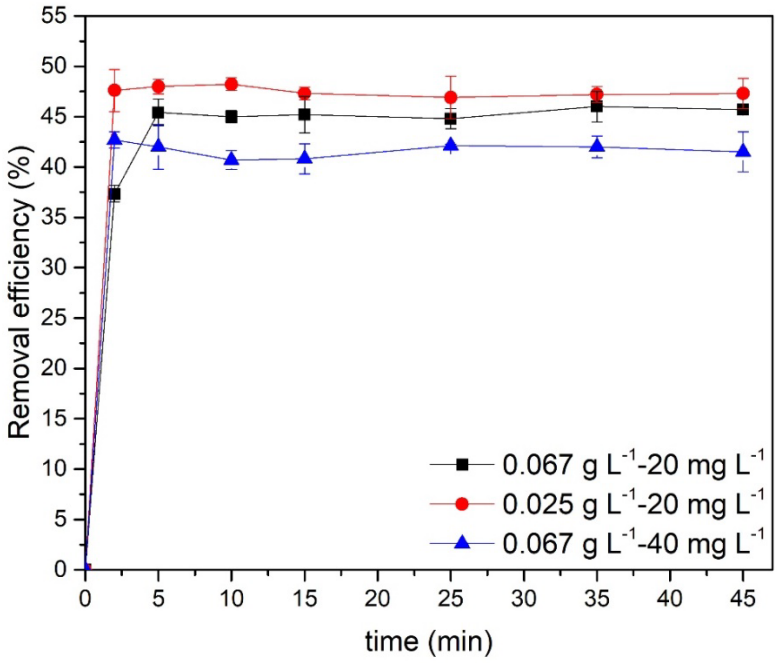


Figure S3: Illustration of the removal efficiency of $NO_3^- - N$ as a function of time for each adsorption experiment performed by using the modified hydrochar ($V = 0.15\ L, pH = 6.5, = 25$ ℃).

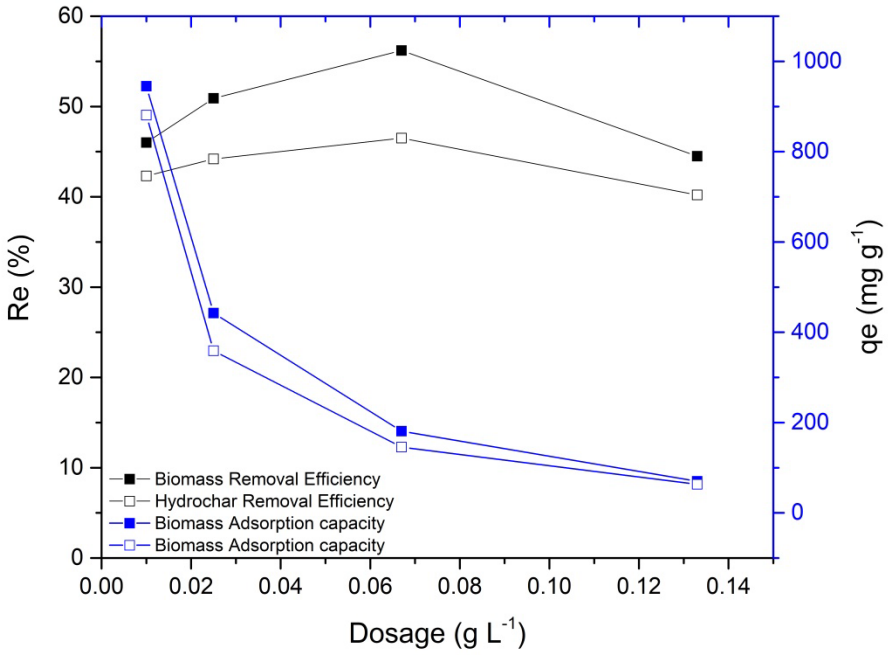


Figure S4: Removal efficiencies paired with adsorption capacities of all examined adsorbent dosages.

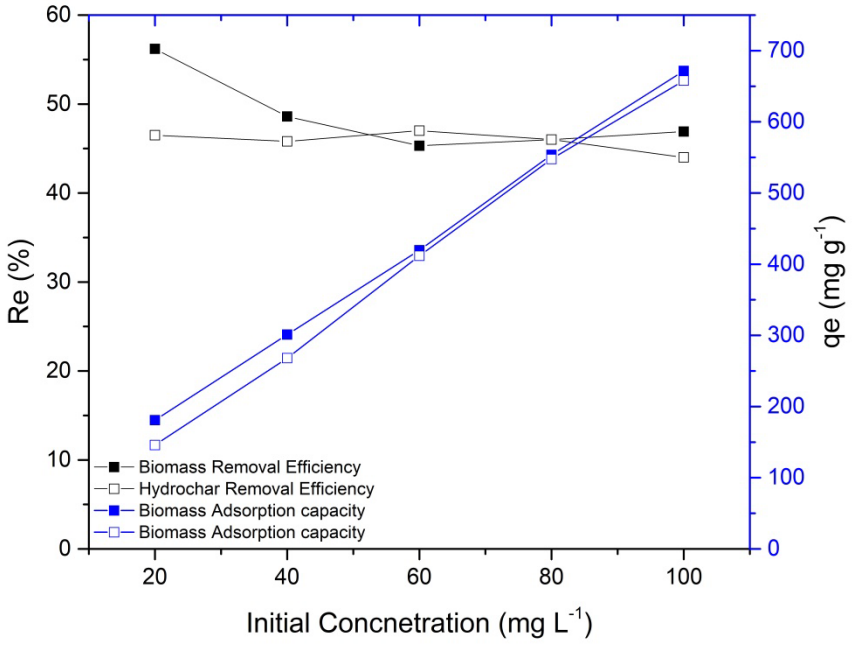


Figure S5: Removal efficiencies paired with adsorption capacities of all examined Initial $NO_3^- - N$ concentrations.

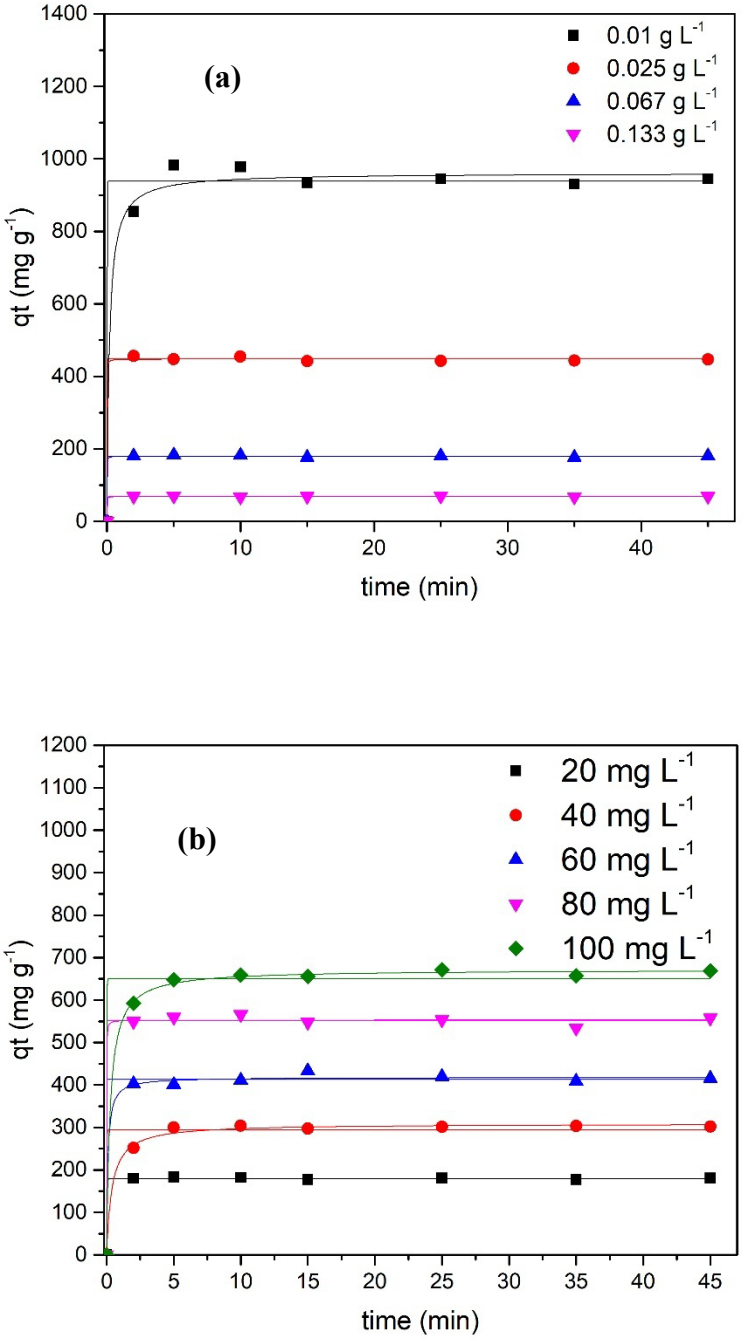


Figure S6: Illustration of the non-linear forms of the pseudo-first-order and pseudo-second-order models: (a) at different adsorption dosages of biomass, and (b) at different initial concentrations of NO_3^--N using biomass as the adsorbent.

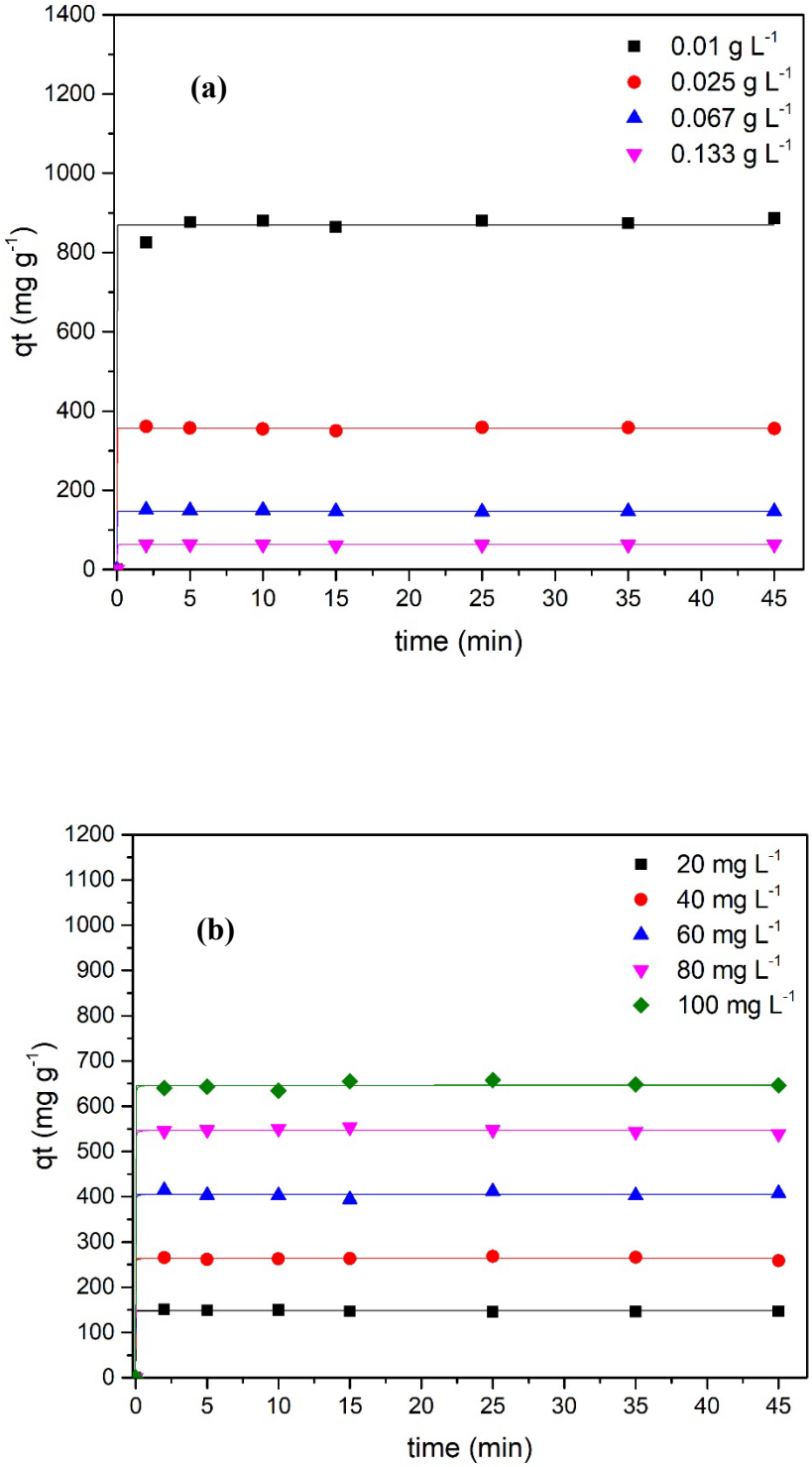


Figure S7: Illustration of the non-linear forms of the pseudo-first-order and pseudo-second-order models: (a) at different adsorption dosages of biomass, and (b) at different initial concentrations of NO_3^--N using hydrochar as the adsorbent.

Table S1: Complete kinetic parameters obtained by non-linear regression for the pseudo-first-order (PFO) and pseudo-second-order (PSO) models. The table presents the correlation coefficient (R^2), residual sum of squares (RSS) (as well as AIC and BIC).

Adsorbent	C_o (mg L^{-1})	Adsorbent dosage ($g\ L^{-1}$)	q_e (exp) ($mg\ g^{-1}$)	Pseudo-second order model					Pseudo-first order model				
				R^2	RSS	$q_e\ (cal)$ ($mg\ g^{-1}$)	k_2 ($g\ mg^{-1}\ min^{-1}$)	AIC/BIC	R^2	RSS	$q_e\ (cal)$ ($mg\ g^{-1}$)	k_1 (min^{-1})	AIC/BIC
Biomass	20 ± 1.0	0.010	945.01	0.986	$1.1 \cdot 10^4$	939.89	-1340004	61.81/ 61.97	0.997	2,668	952.93	1.15	50.47/ 50.63
	20 ± 1.5	0.025	442.62	0.999	$2.1 \cdot 10^2$	448.02	2555276	30.14/ 30.30	0.999	208.1	447.73	41.26	30.07/ 30.23
	20 ± 1.5	0.067	180.82	0.999	34.5	180.50	676507	15.69/ 15.85	0.999	33.1	180.41	6.26	15.36/ 15.52
	20 ± 1.5	0.133	69.83	0.999	6.1	68.94	3688418	1.83/ 1.99	0.999	5.7	68.88	19.94	1.29/ 1.45
	40 ± 1.5	0.067	301.18	0.972	$2 \cdot 10^3$	294.26	-5062532	48.17/ 48.33	0.999	31.3	301.94	0.89	14.91/ 15.07
	60 ± 2.5	0.067	419.70	0.997	$5 \cdot 10^2$	419.26	0.024	37.08/ 37.24	0.996	590.5	415.13	1.75	38.41/ 38.57
	80 ± 1.5	0.067	553.71	0.998	$7 \cdot 10^2$	553.09	13586	39.77/ 39.93	0.998	612.1	553.13	2.52	38.69/ 38.86
	100 ± 6	0.067	671.57	0.989	$4.3 \cdot 10^3$	650.25	-3008920	54.29/ 54.45	0.999	338.4	660.35	1.13	33.96/ 34.12
Hydrochar	20 ± 1.0	0.010	880.98	0.996	$2.6 \cdot 10^3$	869.98	-987624	50.27/ 50.42	0.999	295.9	877.59	1.41	32.88/ 33.04
	20 ± 1.0	0.025	358.97	0.999	76.8	356.76	2135605	22.09/ 22.25	0.999	76.8	356.77	48.37	22.09/ 22.25
	20 ± 1.0	0.067	145.79	0.999	20.6	148.27	2426402	11.57/	0.999	21.8	147.95	38.05	12.02/1

							11.72					2.18
20 ± 1.0	0.133	63.13	0.999	4.8	63.21	$1.8 \cdot 10^7$	0.24/ 0.40	0.999	4.8	63.21	15.28	-0.087/ 0.072
40 ± 1.0	0.067	268.01	0.999	28.5	264.61	1.6	14.16/ 14.32	0.999	58.3	263.28	22.11	19.89/ 20.05
60 ± 1.5	0.067	411.87	0.998	$2.7 \cdot 10^2$	405.50	2132698	32.15/ 32.31	0.999	266.4	405.50	11.51	32.04/ 32.20
80 ± 1.0	0.067	547.72	0.999	86.1	550.36	0.1	23.00/ 23.16	0.999	135.1	546.93	2.92	26.61/ 26.77
100 ± 3.0	0.067	657.99	0.999	$3.9 \cdot 10^2$	652.99	0.03	35.09/ 35.25	0.999	354.6	647.50	2.24	34.33/ 34.49

*As detailed in the main text, the PSO model was not retained for interpretation. Non-linear regression resulted in several non-physical negative values for the rate constant or produced poorly constrained, non-identifiable parameters, confirming the model's inappropriateness for this dataset

Table S2: Parameters for the Langmuir, Freundlich, and Dubinin-Radushkevich isotherm models obtained by non-linear regression for nitrate removal by biomass and hydrochar

Model		Biomass	Hydrochar
Langmuir	R^2	0.974	0.996
	RSS	$3.87 \cdot 10^3$	$7.13 \cdot 10^2$
	$q_{max}\ (mg\ g^{-1})$	4,480	3,998
	$K_L\ (L\ mg^{-1})$	0.0033	0.0036
	AIC/BIC	31.77/29.63	38.09/36.68
Freundlich	R^2	0.981	0.994
	RSS	$2.92 \cdot 10^3$	$1.09 \cdot 10^3$
	n	1.15	1.11
	K_F	21.53	17.78
	AIC/BIC	56.94/54.8	63.26/61.85
Dubinin-Radushkevich	R^2	0.737	0.897
	RSS	$4 \cdot 10^4$	$1.75 \cdot 10^4$
	$K_{DR}\ (mol^2\ kJ^{-2})$	$3.62 \cdot 10^{-5}$	$6.71 \cdot 10^{-5}$
	$q_{max}DR\ (mg\ g^{-1})$	611.41	695.06

*The Langmuir model was not used for interpretation because the experimental data did not exhibit a saturation plateau within the tested concentration range. Consequently, the fitted maximum capacity should be considered a mathematical artifact of extrapolation rather than a physically meaningful value for these materials.

Table S3: Parameters for the Adams-Bohart column adsorption model obtained by non-linear fitting to the initial breakthrough region for biomass and hydrochar fixed-bed columns.

Model		Biomass	Hydrochar
Adams-Bohart	R^2	0.534	0.523
	RSS	1.33	0.96
	$K_{AB}\ (L\ mg^{-1}min^{-1})$	0.00085	0.0006
	$N_o\ (mg\ L_{column}^{-1})$	2,174	2,127

*The Adams-Bohart model is suitable only for describing the initial portion of the breakthrough curve and was not used for full-curve analysis. The Yoon-Nelson model, presented in the main manuscript, was used for overall column performance evaluation